Research Square

Preprints are preliminary reports that have not undergone peer review.
They should not be considered conclusive, used to inform clinical practice,
or referenced by the media as validated information.

PBPK-based exposure–response modeling of enzalutamide and its active metabolite N-desmethyl enzalutamide for the prediction of survival outcomes in patients with prostate cancer

Jeongmin Ha
Ministry of Food and Drug Safety
Hyojin Cho
Chungnam National University
Seongwon Park
Chungnam National University
Woojin Jung
CHA University
Soyoung Lee
Chungnam National University
Hwi-yeol Yun
Chungnam National University
Jung-woo CHAE
jwchae@cnu.ac.kr

Chungnam National University

Article

Keywords:

Posted Date: September 15th, 2026

DOI: https://doi.org/10.21203/rs.3.rs-10913106/v1

License: This work is licensed under a Creative Commons Attribution 4.0 International License.
Read Full License

Additional Declarations:
No competing interests reported.

Tables 1 to 3 are available in the Supplementary Files section.

PBPK-based exposure–response modeling of enzalutamide and its active metabolite N-desmethyl enzalutamide for the prediction of survival outcomes in patients with prostate cancer

Authors

Jeongmin Ha[1#], Hyojin Cho[2#], Seongwon Park[2#], Woojin Jung[3#], Soyoung Lee[2*],Hwi-yeol Yun [2,4,5*], Jung-woo CHAE[2,4,5 *]

[1]Ministry of Food and Drug Safety, Cheongju 28159, Republic of Korea

[2]College of Pharmacy, Chungnam National University, Daejeon 34134, Republic of Korea

[3]Graduate School of Clinical Pharmacy, CHA University, Pocheon 11160, Republic of Korea

[4]Senior Health Convergence Research Center, Chungnam National University, Daejeon 34134, Republic of Korea

[5]Bio-AI Convergence Research Center, Chungnam National University, Daejeon 34134, Republic of Korea

# These authors contributed equally as first authors.

* These authors contributed equally as corresponding authors.

***Corresponding author Information:**

Jung-woo CHAE

College of Pharmacy, Chungnam National University, Daejeon 34134, Republic of Korea

Senior Health Convergence Research Center, Chungnam National University, Daejeon 34134, Republic of Korea

Bio-AI Convergence Research Center, Chungnam National University, Daejeon 34134, Republic of Korea

Email: jwchae@cnu.ac.kr

Tel.: +82-42-821-5929

Abstract
Enzalutamide is an androgen receptor inhibitor extensively metabolized to the pharmacologically active metabolite N-desmethyl enzalutamide. This study developed an integrated physiologically based pharmacokinetic (PBPK) and exposure–response (E–R) modeling framework to evaluate the standard 160-mg and reduced 120-mg once-daily regimens. The whole-body PBPK model demonstrated acceptable predictive performance, with geometric mean fold errors of 1.16–1.35 and mean relative deviations of 1.39–1.41. Virtual population simulations showed that 77.0% and 85.5% of individuals receiving 120 and 160 mg, respectively, achieved the androgen receptor occupancy-associated concentration of 5 μg/mL, whereas 14.5% and 28.5%, respectively, reached or exceeded the exploratory toxicity-associated reference concentration of 16.1 μg/mL. PBPK-predicted total active-moiety trough concentrations were integrated with reconstructed clinical survival data using parametric E–R models. Predicted median progression-free survival was 13.7 and 18.0 months for the 120- and 160-mg regimens, respectively, and predicted median overall survival was 32.0 and 34.0 months. Although the simulation intervals overlapped and the independent exposure effects remained uncertain, the findings provide a model-informed pharmacological rationale for prospective evaluation of reduced-dose enzalutamide as a dose-optimization strategy.

1.Introduction

Enzalutamide is a second-generation androgen receptor (AR) inhibitor that targets the AR signaling pathway. It exerts its antitumor activity by inhibiting androgen binding to the AR, preventing AR nuclear translocation, and blocking AR interaction with DNA.[1,2] Enzalutamide was initially approved in 2012 under the trade name XTANDI® for the treatment of metastatic castration-resistant prostate cancer (mCRPC), with subsequent expansion of its indications to other stages of prostate cancer, including metastatic hormone-sensitive prostate cancer (mHSPC).

The standard approved dosing regimen of enzalutamide is 160 mg once daily. Following oral administration, enzalutamide is absorbed with a time to maximum plasma concentration of approximately 1–2 h and has a long terminal half-life of approximately 5.8 days after a single dose. With once-daily administration, steady state is generally achieved within approximately 4 weeks.[2] Although a high-fat meal may delay the rate of absorption, the overall extent of enzalutamide absorption is not substantially altered. Enzalutamide is highly bound to plasma proteins (approximately 97–98%), while its active metabolite, N-desmethyl enzalutamide, exhibits approximately 95–97% protein binding. Enzalutamide is predominantly metabolized by cytochrome P450 (CYP) enzymes, particularly CYP2C8 and CYP3A4, with CYP2C8 representing the major metabolic pathway.[2,3] N-desmethyl enzalutamide is pharmacologically active and exhibits activity comparable to that of the parent compound, whereas the carboxylic acid metabolite is pharmacologically inactive.[2-5] At steady state, systemic exposure to N-desmethyl enzalutamide is comparable to that of enzalutamide, highlighting the importance of considering both the parent drug and its active metabolite when characterizing enzalutamide pharmacokinetics.

Progression-free survival (PFS) and overall survival (OS) are key clinical efficacy endpoints in prostate cancer. In phase 3 clinical trials, the approved 160-mg daily dose of enzalutamide significantly improved PFS, OS, and other clinically relevant outcomes compared with placebo in patients with advanced prostate cancer.[6–8] However, treatment-related adverse events, including fatigue and central nervous system-related toxicities, can necessitate dose reduction or treatment discontinuation. Several clinical studies have suggested that reduced-dose enzalutamide may retain substantial therapeutic efficacy while improving tolerability, although the exposure-based pharmacological basis supporting such dose-reduction strategies remains insufficiently characterized.[9–14] In particular, it remains unclear whether the additional systemic exposure achieved with the standard 160-mg dose translates into a clinically meaningful improvement in efficacy relative to a reduced dose or instead increases exposure associated with toxicity.

Physiologically based pharmacokinetic (PBPK) modeling provides a mechanistic framework for integrating drug-specific physicochemical and absorption, distribution, metabolism, and excretion properties with physiological characteristics to predict systemic drug exposure under different dosing conditions. Previous PBPK models of enzalutamide and N-desmethyl enzalutamide have primarily focused on the characterization of pharmacokinetics and drug–drug interactions, including CYP2C8- and CYP3A4-mediated interactions.[4] However, the application of PBPK modeling to the quantitative evaluation of alternative enzalutamide dosing strategies has not been sufficiently explored. In particular, integration of PBPK-predicted exposure with pharmacologically relevant target concentrations, exposure associated with toxicity, and long-term clinical efficacy may provide a quantitative framework for evaluating whether a reduced enzalutamide dose can maintain therapeutic benefit while limiting unnecessary systemic exposure.

Therefore, this study aimed to develop and evaluate a whole-body PBPK model for enzalutamide and its active metabolite, N-desmethyl enzalutamide, and to apply the model to quantitatively compare the standard 160-mg and reduced 120-mg once-daily dosing regimens. PBPK-based population simulations were performed to characterize steady-state exposure and pharmacological target attainment, while a previously reported toxicity-associated trough concentration was incorporated as an exploratory safety benchmark. Furthermore, PBPK-derived exposure metrics were integrated with parametric survival models of PFS and OS to characterize the exposure–response relationship.

Through this integrated PBPK and E-R modeling framework, we sought to provide a quantitative pharmacological basis for evaluating reduced-dose enzalutamide as a potential dose-optimization strategy.

2. Methods

2.1. Data & Software

Clinical pharmacokinetic and survival data were obtained from previously published clinical studies. For PBPK model development and evaluation, plasma concentration–time data for enzalutamide and N-desmethyl enzalutamide were collected from single- and multiple-dose studies conducted in healthy participants and patients with prostate cancer.[15] When numerical pharmacokinetic data were not directly available, concentration–time profiles were digitized using WebPlotDigitizer.

For exposure–response (E-R) modeling, published Kaplan–Meier curves for progression-free survival (PFS) and overall survival (OS) were obtained from clinical studies evaluating enzalutamide at the investigated dose levels, including 120 and 160 mg, as well as corresponding placebo groups.[6,8,12,16]

The Kaplan–Meier figures were imported into IPDfromKM, and ordered time–survival probability coordinates were extracted along the entire reported follow-up period rather than at selected time points. The total sample size and the numbers at risk at the reported risk-table time points were entered for each treatment group; the total number of events was additionally incorporated when available. Individual event and censoring times were subsequently reconstructed using the modified iterative Kaplan–Meier algorithm implemented in IPDfromKM (https://biostatistics.mdanderson.org/shinyapps/IPDfromKM/).[19] The accuracy of the reconstruction was assessed by overlaying the reconstructed and published Kaplan–Meier curves and by comparing the reconstructed numbers at risk and survival estimates with the corresponding reported values.

PBPK models for enzalutamide and its active metabolite, N-desmethyl enzalutamide, were developed using PK-Sim® version 11.2 (Open Systems Pharmacology Suite). E-R models were developed using NONMEM version 7.5.1 (ICON Development Solutions, Ellicott City, MD, USA), with Pirana version 3.0.0 and Perl-speaks-NONMEM (PsN) version 5.3.1 used for model execution and evaluation. Data processing, noncompartmental analysis, statistical analyses, target-attainment calculations, and graphical visualization were performed using R version 4.4.1 and RStudio.

2.2. PBPK model development and evaluation

A comprehensive literature search was conducted to collect physicochemical properties, in vitro and in vivo absorption, distribution, metabolism, and excretion (ADME) data, and clinical pharmacokinetic profiles of enzalutamide and N-desmethyl enzalutamide. Drug-specific parameters required for PBPK model development were obtained from published literature and the U.S. Food and Drug Administration (FDA) clinical pharmacology and biopharmaceutics reviews whenever available.[17] Parameters that were not directly available from the literature were estimated or optimized by fitting the model to the observed clinical pharmacokinetic data. For tissue distribution, the specific organ permeability ($P_{eff,\,man}$) was set to 5.15×10^{-4} cm/s based on a previously published study.[2]

The metabolic clearance of enzalutamide was parameterized based on a literature-reported intrinsic clearance (CLint) of 0.894 μL/min/mg protein.[18] Enzalutamide metabolism was represented by four pathways: (1) CYP2C8-mediated formation of N-desmethyl enzalutamide, (2) CYP2C8-mediated metabolism to other metabolites, (3) CYP3A4-mediated formation of N-desmethyl enzalutamide, and (4) CYP3A4-mediated metabolism to other metabolites. The relative contributions of these pathways were determined using clinical drug–drug interaction (DDI) data with gemfibrozil, a potent CYP2C8

inhibitor, and itraconazole, a potent CYP3A4 inhibitor.[4]

Because the intrinsic clearance of N-desmethyl enzalutamide has not been directly reported, its value was derived from the total hepatic clearance reported in a previous PBPK study using an in vitro–in vivo scaling approach (Equations 1 and 2).[4,20]

$$CL_{hepatic} = CL_{int,HLM} \times 32\ \text{MPPGL}^{21} \times 25.7\ (\text{Human liver scaling factor}^{21}) \quad (1)$$

$$CL_{specific} = \frac{CL_{int}}{2.36\ (\text{Volume of liver}) \times 0.67(\text{Fraction intercellular of liver})} \quad (2)$$

To evaluate the predictive performance of the PBPK model, the predicted pharmacokinetic parameters, including C_{max} and AUC_{last}, were compared with their corresponding observed values. The geometric mean fold error (GMFE) for C_{max} and AUC_{last} and the mean relative deviation (MRD) for the plasma concentration–time profiles were calculated according to Equations 3 and 4, respectively. Model performance was considered acceptable when the predicted PK parameters were within two-fold of the corresponding observed values.[21] The MRD and GMFE were calculated as follows:

$$\text{MRD} = 10^{x},\ \text{with}\ x = \sqrt{\frac{1}{m}\sum_{i=1}^{m}\left(\log_{10} C_{pred,i} - \log_{10} C_{obs,i}\right)^{2}} \quad (3)$$

$$\text{GMFE} = 10^{x},\ \text{with}\ x = \frac{1}{n}\sum_{i=1}^{n}\left|\left(\log_{10} PK_{pred,i} - \log_{10} PK_{obs,i}\right)\right| \quad (4)$$

where $C_{pred,i}$ and $C_{obs,i}$ represent the predicted and observed plasma concentrations for the i th observation, respectively, and m represents the total number of concentration pairs. $PK_{pred,i}$ and $PK_{obs,i}$ represent the predicted and observed pharmacokinetic parameters C_{max} or AUC_{last} for the i th comparison, respectively, and n represents the total number of pharmacokinetic parameter pairs. In addition, goodness-of-fit plots were generated to visually compare the predicted and observed plasma concentration–time profiles and pharmacokinetic parameters.

A sensitivity analysis was performed to identify the input parameters that had the greatest influence on the predicted pharmacokinetic profiles of the final PBPK model. Parameters that were optimized during model development or were potentially affected by the selected calculation methods were included in the analysis. The evaluated parameters included lipophilicity, solubility, fraction unbound in plasma, specific intestinal permeability, dissolution time and shape, and clearance parameters associated with enzymatic reactions.

2.3. PBPK-based pharmacological target attainment analysis

Virtual population simulations were performed using the final PBPK model to characterize the steady-state trough concentration ($C_{trough,\,ss}$) of enzalutamide following once-daily administration of 120 and 160 mg. For each dosing regimen, 200 virtual individuals were generated based on the demographic characteristics of the patient population represented in the clinical survival studies.[6,8,12,16] This population size was selected in accordance with previous PBPK simulation studies that used 200 virtual individuals to characterize population-level pharmacokinetic variability and exposure distributions.[21,22,23]

Pharmacological target attainment was evaluated using a $C_{trough,ss}$ of 5 μg/mL as a pharmacologically relevant benchmark, based on previous FDHT-PET findings suggesting near-maximal androgen receptor occupancy at concentrations around this level.[2,23] Target attainment was defined as an

individual $C_{trough,ss} \geq 5$ μg/mL, and the target attainment rate (TAR) was calculated as the proportion of virtual individuals achieving this benchmark.

For additional clinical context, the simulated $C_{trough, ss}$ distributions were also considered in relation to a previously reported toxicity-associated concentration. Patients requiring dose reduction because of Grade 3 toxicity had a higher mean enzalutamide Ctrough than those not requiring dose reduction (16.1 ± 2.4 vs. 11.6 ± 2.6 μg/mL; P = 0.027).[24] The reported value of 16.1 μg/mL was therefore used only as an exploratory reference for contextualizing the upper range of the simulated exposure distributions and not as a formal toxicity threshold.

2.4. E-R Model development and evaluation

Parametric survival models were developed to characterize progression-free survival (PFS) and overall survival (OS). Prior to the incorporation of exposure covariates, four parametric survival distributions—exponential (Equation 5), Weibull (Equation 6), Gompertz (Equation 7), and log-normal (Equation 8)—were evaluated as candidate base structural models. The optimal structural model for each survival endpoint was selected based on the Akaike information criterion (AIC).

$$S(t) = \exp^{-\lambda t} \tag{5}$$

$$S(t) = \exp^{-\lambda \gamma t^{\gamma-1}} \tag{6}$$

$$S(t) = \exp^{-\lambda t \gamma} \tag{7}$$

$$S(t) = 1 - \emptyset\left(\frac{\ln t - \mu}{\sigma}\right) \tag{8}$$

where S(t) denotes the probability of remaining event-free beyond time t; λ denotes the scale or rate parameter; γ denotes the shape parameter for the Weibull and Gompertz distributions; and μ and σ denote the location and scale parameters, respectively, of the logarithm of survival time in the log-normal distribution.

Following selection of the base structural model, PBPK-predicted $C_{trough, ss}$ was selected as the representative exposure metric for the E–R analysis. This selection was pharmacologically motivated by FDHT-PET findings indicating that enzalutamide-mediated androgen receptor target engagement approached a plateau over the clinically relevant trough-concentration range.[23] In addition, $C_{trough, ss}$ has been used as an exposure metric in a large exposure–response analysis of overall survival and in smaller clinical studies evaluating exposure in relation to pharmacological activity or toxicity.[2,25] Collectively, these pharmacological and clinical considerations supported the selection of $C_{trough, ss}$ as the representative exposure metric in the present analysis.

Because N-desmethyl enzalutamide is pharmacologically active and exhibits key primary pharmacodynamic activity of similar in vitro potency to that of enzalutamide, the trough concentrations of the parent drug and active metabolite were summed assuming equal potency to derive total active-moiety $C_{trough, ss}$.[2] This 1:1 potency assumption was used as a pragmatic approximation because compound-specific clinical potency estimates were not available.

The resulting total active-moiety C_{trough} was incorporated into the hazard model as a continuous, time-varying covariate and centered relative to the median value within each active-dose group. The categorical effects of the 120- and 160-mg dosing regimens were also evaluated. Models incorporating the Ctrough effect, categorical dose effect, or both effects were assessed to determine whether PBPK-predicted exposure provided additional information beyond the administered dose. Model selection was based on an integrated assessment of numerical and graphical criteria. Numerical evaluation included changes in the objective function value (OFV), parameter precision, and parameter uncertainty, while visual assessment was performed by comparing the observed and model-

predicted survival profiles and examining the corresponding time-to-event visual predictive checks (VPCs).

The robustness and parameter uncertainty of the final E-R models were assessed using a nonparametric bootstrap with 1,000 resampling iterations, from which 95% confidence intervals (CIs) for the model parameters were obtained. VPCs based on 1,000 simulations were additionally performed to evaluate the ability of the final models to reproduce the observed PFS and OS profiles.

3. Results

3.1. Data characteristics

A total of eight clinical datasets were used for the development and evaluation of the PBPK models of enzalutamide and N-desmethyl enzalutamide. The enzalutamide datasets covered single oral doses ranging from 30 to 360 mg and once-daily multiple-dose regimens ranging from 30 to 360 mg. The study populations included healthy participants, patients with castration-resistant prostate cancer (CRPC), and patients with hormone-naïve prostate cancer (HNPC), and included both Caucasian and Asian populations. Detailed characteristics of the clinical datasets are summarized in Supplementary Table S1.

For the E-R analysis, published survival data were obtained from four clinical studies evaluating enzalutamide in patients with prostate cancer. The survival datasets included 120-mg and 160-mg enzalutamide regimens as well as placebo groups, where available, and comprised patients with CRPC, metastatic CRPC (mCRPC), and metastatic hormone-sensitive prostate cancer (mHSPC). Both Asian and Caucasian populations were represented. Published PFS and OS profiles were reconstructed for subsequent parametric survival modeling, and the characteristics of the clinical survival datasets are summarized in Supplementary Table S3.

3.2. PBPK Model development and evaluation

A whole-body PBPK model of enzalutamide and its active metabolite N-desmethyl enzalutamide was developed. The initial and final drug-specific parameters used in the PBPK model are summarized in Table 1. Based on the implemented CYP2C8- and CYP3A4-mediated metabolic pathways, the final intrinsic clearance values for the formation of N-desmethyl enzalutamide and other metabolites were 0.11 and 0.02 L/min, respectively, for CYP2C8, and 0.00261 and 0.01 L/min, respectively, for CYP3A4. The final hepatic clearance of N-desmethyl enzalutamide was 0.18 mL/min/kg. The CYP2C8-mediated pathway, which accounted for 87% of the overall metabolic clearance of enzalutamide, was further divided into the formation of N-desmethyl enzalutamide (67%) and other metabolites (33%). Similarly, the CYP3A4-mediated pathway, accounting for the remaining 13% of the overall metabolic clearance, was divided into N-desmethyl enzalutamide formation (39%) and other metabolic pathways (61%).

Sensitivity analysis was performed based on AUClast following multiple-dose administration of enzalutamide for 175 days. For enzalutamide, fraction unbound in plasma, lipophilicity (LogP), and CYP2C8-mediated intrinsic clearance for the formation of N-desmethyl enzalutamide showed the greatest influence on the predicted AUClast. For N-desmethyl enzalutamide, the most influential parameters were its fraction unbound in plasma and total hepatic clearance, as well as the lipophilicity of enzalutamide (Figure S3).

The final PBPK model adequately described the observed plasma concentration–time profiles of enzalutamide and N-desmethyl enzalutamide following both single- and multiple-dose administration (Figures S1 and S2). The mean predicted-to-observed ratios for C_{max} and AUC_{last} were 0.93 and 0.85, respectively, for enzalutamide and 0.79 and 0.77, respectively, for N-desmethyl enzalutamide. The corresponding GMFE values for C_{max} were 1.16 and 1.29, and those for AUC_{last} were 1.27 and 1.35,

respectively. Individual observed and predicted Cmax and AUClast values for each clinical dataset are provided in Table S2.

Overall, 89.2% and 90.1% of the predicted plasma concentrations of enzalutamide and N-desmethyl enzalutamide, respectively, were within two-fold of the corresponding observed concentrations. The overall MRD values were 1.39 for enzalutamide and 1.41 for N-desmethyl enzalutamide, indicating acceptable predictive performance of the final PBPK model. The GOF plots comparing the predicted and observed plasma concentrations and PK parameters are presented in Figure 2.

3.3. PBPK-based pharmacological target attainment analysis

PBPK-based virtual population simulations showed a dose-dependent increase in steady-state enzalutamide trough concentrations ($C_{\text{trough, ss}}$) from 120 to 160 mg once daily (Figure 3). Of the 200 virtual individuals in each dosing group, 77.0% (154/200) at 120 mg and 85.5% (171/200) at 160 mg achieved the predefined pharmacologically relevant concentration of $C_{\text{trough, ss}} \geq 5\mu g/mL$.

For additional clinical context, 14.5% (29/200) of individuals receiving 120 mg and 28.5% (57/200) of those receiving 160 mg had $C_{\text{trough, ss}} \geq 16.1\mu g/mL$, a previously reported mean concentration in patients requiring dose reduction because of Grade 3 toxicity. Accordingly, 62.5% (125/200) and 57.0% (114/200) of individuals in the 120- and 160-mg groups, respectively, had $C_{\text{trough, ss}}$between 5 and 16.1 µg/mL. Thus, the 160-mg regimen produced a higher pharmacological target-attainment rate, while also resulting in a greater proportion of simulated individuals with exposures at or above the exploratory toxicity-associated reference concentration. This comparison was intended to contextualize the simulated exposure distributions and does not establish 16.1 µg/mL as a toxicity threshold.

3.4. E-R Model development and evaluation

Among the candidate parametric survival distributions, the Weibull model had the lowest Akaike information criterion (AIC) for PFS, whereas the log-normal model had the lowest AIC for OS. Accordingly, the Weibull and log-normal distributions were selected as the base structural models for PFS and OS, respectively.

The addition of both the categorical dose-group effect and PBPK-predicted total active-moiety C_{trough}produced the greatest improvement relative to the respective base structural models. The OFV decreased from 4,213 to 4,075 for PFS (ΔOFV = −138) and from 9,961 to 9,942 for OS (ΔOFV = −19). The combined models also provided better graphical agreement with the reconstructed survival profiles than the base models or models incorporating either effect alone and were therefore selected as the final E–R models. In both models, the estimated C_{trough}-effect parameter indicated that increasing total active-moiety $C_{\text{trough}}$was associated with reductions in the progression and mortality hazards. The direction of the estimated exposure effects was therefore consistent with the expected pharmacological effect of enzalutamide.

The parameter estimates from the final PFS and OS models were generally comparable with the median estimates obtained from 1,000 nonparametric bootstrap replicates. However, the exposure-effect parameters were estimated with relatively low precision and had wide bootstrap confidence intervals that included zero, indicating uncertainty in the magnitude of the independent exposure–survival relationships. The final parameter estimates, relative standard errors, bootstrap medians, and corresponding 95% confidence intervals are presented in Tables 2 and 3.

Time-to-event VPCs based on 1,000 simulations showed that the final models adequately captured the overall survival patterns across the placebo, 120-mg, and 160-mg groups (Figures 4 and 5). For PFS, the model-predicted median survival times were 13.7 months (95% simulation interval, 8.7–20.0) for

the 120-mg group and 18.0 months (95% simulation interval, 11.0–25.0) for the 160-mg group, compared with 6.8 months for the placebo group. For OS, the corresponding median survival times were 32.0 months (95% simulation interval, 22.0–50.0) and 34.0 months (95% simulation interval, 32.0–36.0), respectively, compared with 26.4 months for the placebo group. Although the point estimates were numerically higher with 160 mg, particularly for PFS, the simulation intervals overlapped between the active-dose groups. Overall, the model-predicted survival profiles were generally consistent with the reconstructed observed data, although prediction uncertainty increased at later time points.

4. Discussion

In this study, the relationship between systemic exposure to enzalutamide and its active metabolite, N-desmethyl enzalutamide, and clinical efficacy was quantitatively evaluated across different dosing regimens. The whole-body PBPK model successfully characterized the pharmacokinetics of enzalutamide and its active metabolite, N-desmethyl enzalutamide, and enabled prediction of steady-state exposure across clinically relevant doses. By integrating PBPK-predicted exposure with pharmacological target attainment and parametric survival models for PFS and OS, the present study provided a quantitative framework for comparing the standard 160-mg dose with the reduced 120-mg dose. Overall, the results suggest that the increase in systemic exposure achieved with 160 mg may not translate proportionally into additional clinical benefit, supporting further investigation of reduced-dose enzalutamide as a potential dose-optimization strategy.

The metabolic pathways and clearance characteristics estimated in the final PBPK model were generally consistent with the previously reported disposition of enzalutamide and N-desmethyl enzalutamide.[17-20] Enzalutamide was predominantly metabolized through CYP2C8, with a smaller contribution from CYP3A4, consistent with previous clinical pharmacology and DDI studies. In addition, the hepatic clearance estimated for N-desmethyl enzalutamide was comparable in magnitude to previously reported values, supporting the physiological plausibility of the disposition parameters implemented in the model.[2,4,18] The model also adequately characterized enzalutamide pharmacokinetics across a broad dose range. This is consistent with previous clinical pharmacokinetic findings showing approximately dose-proportional exposure over the clinically investigated dose range.[2] The ability of the model to reproduce exposure across both single- and multiple-dose studies therefore supports its application to the subsequent comparison of the 120- and 160-mg regimens. The clinical datasets used for model development and evaluation included populations with different ethnic backgrounds, and no systematic ethnicity-related bias was apparent in the overall model performance. This observation is consistent with previous clinical pharmacokinetic evaluations indicating that race does not have a clinically meaningful effect on enzalutamide exposure.[2,17]

Sensitivity analysis identified the fraction unbound in plasma, lipophilicity, CYP2C8-mediated intrinsic clearance, and dissolution characteristics as major determinants of enzalutamide exposure. Among these parameters, CYP2C8-mediated clearance is mechanistically consistent with the established predominant role of CYP2C8 in enzalutamide metabolism. Although the fraction unbound was adjusted during model development and exhibited relatively high sensitivity, the final parameterization enabled the model to adequately reproduce enzalutamide exposure across a wide range of single- and multiple-dose clinical studies. For N-desmethyl enzalutamide, exposure was particularly sensitive to its fraction unbound and total hepatic clearance. Because detailed enzyme-specific information regarding the elimination of N-desmethyl enzalutamide was limited, its elimination was represented using total hepatic clearance. The high sensitivity to this parameter therefore represents an important source of uncertainty in the metabolite model. Nevertheless, the final model adequately reproduced the observed N-desmethyl enzalutamide concentration–time profiles and exposure metrics, supporting its application for subsequent exposure simulations.

PBPK population simulations provided further insight into the pharmacological implications of dose reduction from 160 to 120 mg. Although the standard 160-mg regimen resulted in higher steady-state trough concentrations, 77.0% of individuals receiving 120 mg achieved a $C_{trough,\ ss} \geq 5$ μg/mL, compared with 85.5% of those receiving 160 mg. This finding suggests that the lower systemic exposure achieved with 120 mg may still be sufficient to maintain substantial AR inhibition in a large proportion of patients, while the incremental gain in pharmacological target attainment with 160 mg was relatively modest.

The simulated exposure distributions were additionally compared with a previously reported mean C_{trough} of 16.1 μg/mL in patients requiring dose reduction because of Grade 3 toxicity.[24] The proportion of virtual individuals with concentrations at or above this exploratory reference value increased from 14.5% at 120 mg to 28.5% at 160 mg. Together with the relatively modest increase in pharmacological target attainment from 77.0% to 85.5%, this finding suggests a potential trade-off between incremental AR target attainment and the increased occurrence of relatively high exposure at the 160-mg dose. Although 16.1 μg/mL does not represent a validated toxicity threshold, these exploratory results support further investigation of the exposure–tolerability relationship across the clinically used dose range.[9-14]

PBPK-predicted steady-state trough concentration ($C_{trough,\ ss}$) was prespecified as the representative exposure metric because it can be assessed using a clinically feasible predose sample and represents the systemic drug concentration maintained at the end of the dosing interval, and has previously been evaluated in relation to enzalutamide-mediated AR target engagement and survival outcomes.[2,23,24] Simulations based on the final models incorporating both dose-group and $C_{trough,\ ss}$ effects yielded median PFS estimates of 13.7 months with 120 mg and 18.0 months with 160 mg, with corresponding 95% simulation intervals of 8.7–20.0 and 11.0–25.0 months, respectively. The predicted median OS estimates were 32.0 and 34.0 months for the 120- and 160-mg regimens, respectively, with 95% simulation intervals of approximately 22.0–50.0 and 32.0–36.0 months. Although the point estimates were numerically higher with 160 mg, particularly for PFS, the predicted intervals overlapped substantially between the two active-dose groups, and the OS estimates were similar. Thus, the higher $C_{trough,\ ss}$ achieved with 160 mg did not result in clearly distinguishable survival improvement relative to 120 mg. These findings are consistent with a relatively shallow exposure–efficacy relationship over the clinically relevant exposure range, although they should not be interpreted as demonstrating therapeutic equivalence between the two regimens because the exposures were PBPK-predicted rather than individually observed and matched to the reconstructed survival outcomes.

From a benefit–risk perspective, the combined findings provide a pharmacological rationale for further evaluation of 120 mg as a dose-optimization strategy. Dose optimization does not necessarily require maximizing systemic exposure, particularly when pharmacological target engagement approaches saturation and further increases in exposure may predominantly increase the risk of toxicity. In the present analysis, the lower exposure achieved with 120 mg was accompanied by substantial AR target attainment, a lower proportion of individuals reaching toxicity-associated concentrations, and modeled survival outcomes that did not indicate a clear proportional efficacy gain with the higher 160-mg exposure. These findings therefore support 120 mg as a potentially favorable dose for balancing efficacy and tolerability, rather than establishing it as a universally optimal dose or as clinically noninferior to 160 mg. Prospective clinical evaluation is warranted to determine whether this model-informed benefit–risk advantage translates into improved tolerability while maintaining clinical efficacy.

The current FDA-approved recommended dose of enzalutamide is 160 mg once daily; however, dose reduction to 120 or 80 mg is permitted for patients experiencing Grade ≥3 or intolerable adverse reactions.[25] Thus, 120 mg represents a clinically recognized dose-reduction level, although it is not currently recommended as the standard starting dose. The present findings provide a pharmacological rationale for prospectively evaluating whether this reduced dose could achieve a more favorable benefit–risk balance in selected patients. This concept is aligned with the FDA's Project Optimus and its recent guidance on oncology dose optimization, which emphasize integrating efficacy, safety,

tolerability, pharmacodynamic information, and exposure–response relationships when selecting an optimized dosage.[26] Accordingly, the present PBPK–E-R framework should not be interpreted as evidence for replacing the currently approved 160-mg starting dose, but rather as a model-informed rationale for prospective evaluation of reduced-dose strategies.

Several limitations should be acknowledged. First, clinical evidence directly comparing reduced-dose enzalutamide with the standard 160-mg regimen remains limited, particularly for doses below 120 mg. Although the present analyses suggest that 120 mg may maintain pharmacologically relevant exposure, the substantial overlap between the predicted survival intervals for the 120- and 160-mg regimens should not be interpreted as demonstrating therapeutic equivalence or noninferiority. Prospective dose-ranging studies are required to confirm the efficacy and tolerability of reduced-dose regimens.

Second, the datasets used for E–R modeling lacked individual-level demographic characteristics, including race and body size, as well as original patient-level PK and survival data that were directly linked at the individual level. Consequently, PBPK-simulated exposure profiles could not be uniquely matched to the patients represented in the reconstructed survival data, and potentially relevant demographic and disease-related prognostic factors could not be incorporated into the survival models. This limited individual-level exposure–outcome linkage reduced the information available for estimating the independent C_{trough} effects and may partly explain their high RSEs and wide bootstrap confidence intervals. Furthermore, from a pharmacological perspective, the wide confidence intervals spanning zero may reflect a true plateau in the exposure–response relationship, wherein androgen receptor saturation is largely attained at concentrations achieved with 120 mg, resulting in a negligible incremental survival benefit with further exposure escalation. In the absence of individually observed PK data, the mechanistic PBPK framework was used to generate biologically informed population-level exposure distributions based on physiological determinants of pharmacokinetics and the demographic characteristics reported for the corresponding clinical populations. This approach did not correct for the absence of directly matched individual data but enabled an exploratory integration of population-level exposure predictions with reconstructed survival outcomes. Accordingly, the estimated exposure–survival associations should be interpreted as hypothesis-generating rather than as definitive individual-level E–R relationships. Prospective studies collecting directly matched individual demographic, PK, efficacy, and survival data will be required to validate the present findings and support further refinement and development of the proposed modeling framework.

Finally, total active-moiety C_{trough} was calculated by assuming comparable pharmacological contributions of enzalutamide and N-desmethyl enzalutamide. Although this assumption was supported by their similar in vitro AR-inhibitory activity, potential differences in their in vivo potency were not explicitly characterized. A direct toxicity E–R model could not be developed because longitudinal individual-level PK and adverse-event data were unavailable. The reported concentration of 16.1 μg/mL was therefore used only as an exploratory toxicity-associated reference for contextualizing the simulated exposure distributions, rather than as a validated toxicity threshold. Future studies incorporating directly matched individual PK, efficacy, and longitudinal safety data are needed to characterize the exposure–benefit–risk relationship and evaluate reduced-dose strategies prospectively.In conclusion, the integrated PBPK and E-R modeling framework successfully characterized the pharmacokinetics of enzalutamide and N-desmethyl enzalutamide and linked PBPK-predicted active exposure with PFS and OS. Although the 160-mg regimen produced greater systemic exposure than the 120-mg regimen, the incremental increase in exposure was associated with limited additional modeled survival benefit, while higher exposure may increase the risk of clinically relevant toxicity. Together with pharmacological target-attainment analysis, these findings provide a model-informed rationale for further prospective evaluation of 120 mg once daily as a potential enzalutamide dose-optimization strategy.

Acknowledgements

This study was supported by Chungnam National University, Institute of Information & Communications Technology Planning Evaluation (IITP) grant funded by the Korea government (MSIT) (No.RS-2022-00155857, Artificial Intelligence Convergence Innovation Human Resources Development (Chungnam National University)); the National Research Foundation of Korea (NRF) grant funded by the Korea government (MSIT; No. RS-2023-00278597, RS-2022-NR070856 [Senior Health Convergence Research Center based on Life Cycle (Chungnam National University)]); the Basic Science Research Program through the National Research Foundation of Korea (NRF) founded by the Ministry of Education (RS-2025-25397599); the Korea Environmental Industry & Technology Institute (KEITI) through Core Technology Development Project for Environmental Diseases Prevention and Management funded by the Korea Ministry of Environment (MOE) (RS-2021-KE001333); a grant from the Korea Machine Learning Ledger Orchestration for Drug Discovery Project (K-MELLODDY) funded by the Ministry of Health & Welfare and Ministry of Science and ICT, Republic of Korea (RS-2024-00460694); the Korea Institute of Toxicology (KIT) Research Program (No. 2710008763, KK-2401-01); the Korea Health Technology R&D Project through the Korea Health Industry Development Institute (KHIDI) grant funded by the Ministry of Health & Welfare, Republic of Korea (grant number: RS-2024-00336984, RS-2025-02306055), support from the Ministry of Trade, Industry, and Energy (MOTIE), Korea, under the “Infrastructure program for industrial innovation” supervised by the Korea Institute for Advancement of Technology (KIAT) (RS-2024-00434342); and a grant (No. 26212MFDS008) from the Ministry of Food and Drug Safety (MFDS), Republic of Korea.

Reference

1. Tran C, Ouk S, Clegg NJ, et al. Development of a second-generation antiandrogen for treatment of advanced prostate cancer. Science. 2009;324(5928):787-90.
2. Gibbons JA, Ouatas T, Krauwinkel W, et al. Clinical Pharmacokinetic Studies of Enzalutamide. Clin Pharmacokinet. 2015;54(10):1043-55.
3. Benoist GE, Hendriks RJ, Mulders PF, et al. Pharmacokinetic Aspects of the Two Novel Oral Drugs Used for Metastatic Castration-Resistant Prostate Cancer: Abiraterone Acetate and Enzalutamide. Clin Pharmacokinet. 2016;55(11):1369-80.
4. Otsuka Y, Poondru S, Bonate PL, et al. Physiologically-based pharmacokinetic modeling to predict drug-drug interaction of enzalutamide with combined P-gp and CYP3A substrates. J Pharmacokinet Pharmacodyn. 2023;50(5):365-76.
5. Krauwinkel W, Noukens J, van Dijk J, et al. A comparison of the pharmacokinetics and safety of enzalutamide in subjects with hepatic impairment and matched healthy subjects. J Clin Pharm Ther. 2017;42(3):268-75.
6. Scher HI, Fizazi K, Saad F, et al. Increased survival with enzalutamide in prostate cancer after chemotherapy. N Engl J Med. 2012;367(13):1187-97.
7. Hussain M, Fizazi K, Saad F, et al. Enzalutamide in Men with Nonmetastatic, Castration-Resistant Prostate Cancer. N Engl J Med. 2018;378(26):2465-74.
8. Beer TM, Armstrong AJ, Rathkopf DE, et al. Enzalutamide in metastatic prostate cancer before chemotherapy. N Engl J Med. 2014;371(5):424-33.
9. Terada N, Akamatsu S, Okada Y, et al. Factors predicting efficacy and adverse effects of enzalutamide in Japanese patients with castration-resistant prostate cancer: results of retrospective multi-institutional study. Int J Clin Oncol. 2016;21(6):1155-61.
10. Boerrigter E, Havenith T, van Erp NP, Schnog JB. Deep and ongoing response of castrate-resistant prostate cancer on very low-dose enzalutamide in an elderly chemotherapy-naive patient: a case report. Cancer Chemother Pharmacol. 2021;88(1):165-8.
11. Bromley HL, Varughese M, Gilbert DC, et al. Comparison of standard-dose and reduced-dose treatment of metastatic prostate cancer with enzalutamide, apalutamide or darolutamide: a rapid review. BMJ Oncology. 2024;3(1).
12. Boerrigter E, Overbeek JK, Benoist GE, et al. A Prospective Randomised Trial to

Determine the Effect of a Reduced Versus Standard Dose of Enzalutamide on Side Effects in Frail Patients with Prostate Cancer. Eur Urol Oncol. 2024;7(6):1376-83.
13. Vinh-Hung V, Natchagande G, Joachim C, et al. Low-Dose Enzalutamide in Late-Elderly Patients (>/= 75 Years Old) Presenting With Metastatic Castration-Resistant Prostate Cancer. Clin Genitourin Cancer. 2020;18(6):e660-e8.
14. Vinh-Hung V, Gorobets O, Natchagande G, et al. Low-Dose Enzalutamide in Metastatic Prostate Cancer-Longevity Over Conventional Survival Analysis. Clin Genitourin Cancer. 2022;20(6):e473-e84.
15. Liu YM, Wu P, Fukushi R, Yamada S, Chen Q. Pharmacokinetics and Safety of Enzalutamide in Healthy Chinese Male Volunteers. Clin Ther. 2019;41(2):261-8.
16. Tsuzuki S, Nakanishi S, Tamaki M, et al. Initial dose reduction of enzalutamide does not decrease the incidence of adverse events in castration-resistant prostate cancer. PLoS One. 2021;16(10):e0258160.
17. XTANDI®: Clinical Pharmacology and Biopharmaceutics Review(s). https://www.accessdata.fda.gov/drugsatfda_docs/nda/2012/203415Orig1s000ClinPharmR.pdf Accessed Oct 11, 2024.
18. Jiang J, Pang X, Li L, et al. Effect of N-methyl deuteration on metabolism and pharmacokinetics of enzalutamide. Drug Des Devel Ther. 2016;10:2181-91.
19. Liu N, Zhou Y, Lee JJ. IPDfromKM: reconstruct individual patient data from published Kaplan–Meier survival curves. BMC Med Res Methodol. 2021;21:111. doi:10.1186/s12874-021-01308-8.
20. Khojasteh SC, Wong H, Hop CECA, eds. *Drug Metabolism and Pharmacokinetics Quick Guide*. Springer; 2011:127-140.
21. Jones HM, Chen Y, Gibson C, et al. Physiologically based pharmacokinetic modeling in drug discovery and development: a pharmaceutical industry perspective. Clin Pharmacol Ther. 2015;97(3):247-62.
22. Gerhart JG, Carreño FO, Edginton AN, et al. Development and evaluation of a virtual population of children with obesity for physiologically based pharmacokinetic modeling. Clin Pharmacokinet. 2022;61(2):307–20. doi:10.1007/s40262-021-01072-4.
23. Scher, H. I. et al. Antitumour activity of MDV3100 in castration-resistant prostate cancer: a phase 1–2 study. *Lancet* **375**, 1437–1446 (2010)
24. Joulia ML, Carton E, Jouinot A, et al. Pharmacokinetic/pharmacodynamic relationship of enzalutamide and its active metabolite N-desmethyl enzalutamide in metastatic castration-resistant prostate cancer patients. *Clin Genitourin Cancer.* 2020;18(2):155–160. doi:10.1016/j.clgc.2019.05.020.
25. U.S. Food and Drug Administration. *XTANDI (enzalutamide) capsules, for oral use; XTANDI (enzalutamide) tablets, for oral use: Prescribing Information.* Revised March 2025.
26. U.S. Food and Drug Administration. *Optimizing the Dosage of Human Prescription Drugs and Biological Products for the Treatment of Oncologic Diseases: Guidance for Industry.* Silver Spring, MD: U.S. Food and Drug Administration; 2024.

Role of the Funders/Sponsors: The funding organizations had no role in the design or conduct of the study; collection, management, analysis, or interpretation of the data; preparation, review, or approval of the manuscript; or the decision to submit the manuscript for publication.

Competing Interests

The authors declare no financial or non-financial competing interests.

Data Availability

The data analyzed in this study were obtained from publicly available published studies. Plasma concentration–time data and Kaplan–Meier survival curves were digitized or reconstructed from the cited publications. The processed datasets generated during the current study are available from the corresponding author upon reasonable request.

Code Availability

The custom code and model files used in this study are available from the corresponding author upon reasonable request.

Author Contributions

J.H., H.C., S.P., and W.J. contributed equally to this work. J.H., H.C., S.P., W.J., S.L., H.Y., and J.C. contributed to the conceptualization and design of the study. J.H. and H.C. performed data collection, data reconstruction, pharmacokinetic modeling, exposure–response analysis, and visualization. S.P. and W.J. contributed to the methodology, validation, and interpretation of the results. J.H., H.C., S.P., and W.J. drafted the manuscript. S.L., H.Y., and J.C. supervised the study and critically revised the manuscript for important intellectual content. H.Y. and J.C. acquired funding and provided project administration. All authors reviewed and approved the final version of the manuscript.

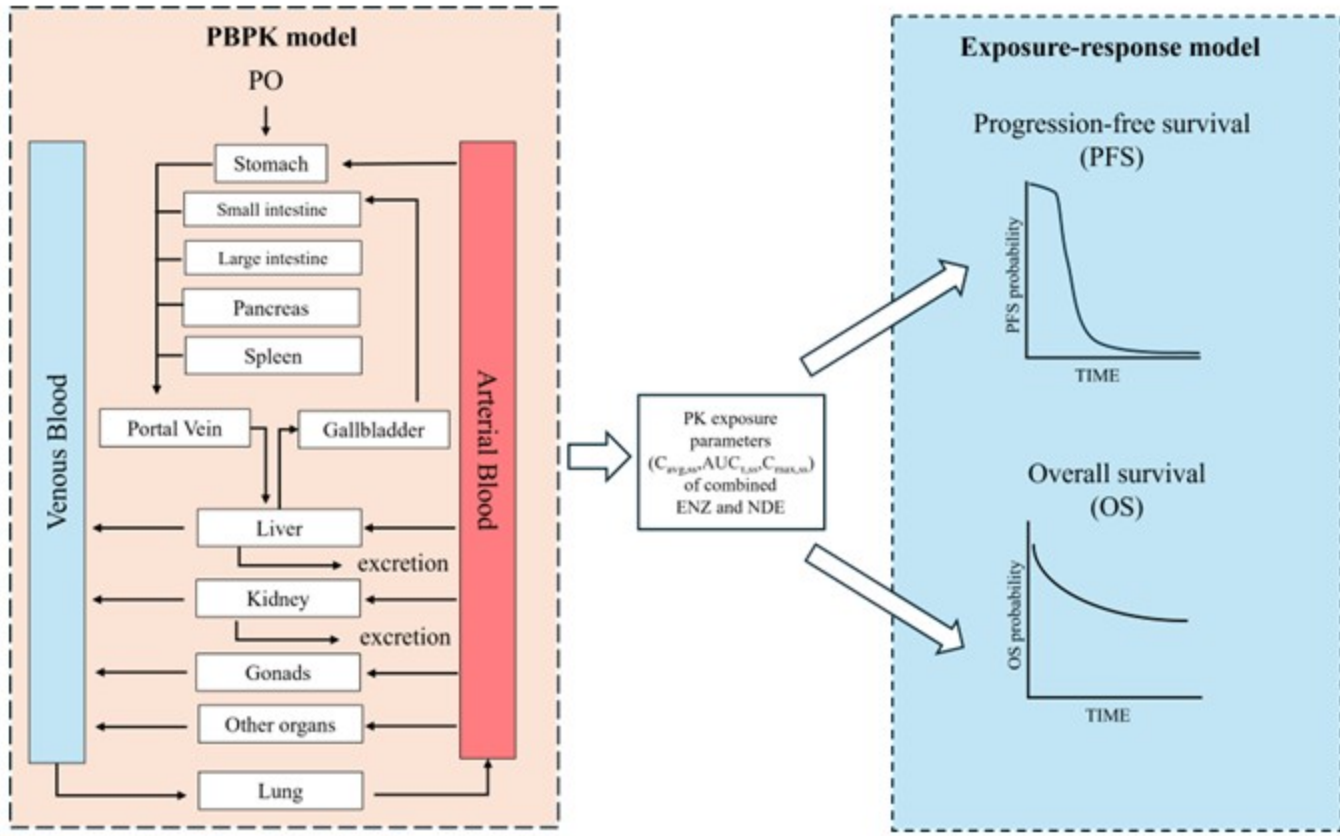


FIGURE1
Schematic representation of the physiologically based pharmacokinetic (PBPK) based exposure-response model. PO, per oral; PK, Pharmacokinetic; $C_{avg,ss}$, average value of plasma concentration in steady state; $AUC_{t,ss}$, area under the 24-hour interval curve of plasma concentration in steady state; $C_{max,ss}$, maximum value of plasma concentration in steady state; ENZ, Enzalutamide; NDE, N-desmethyl enzalutamide.

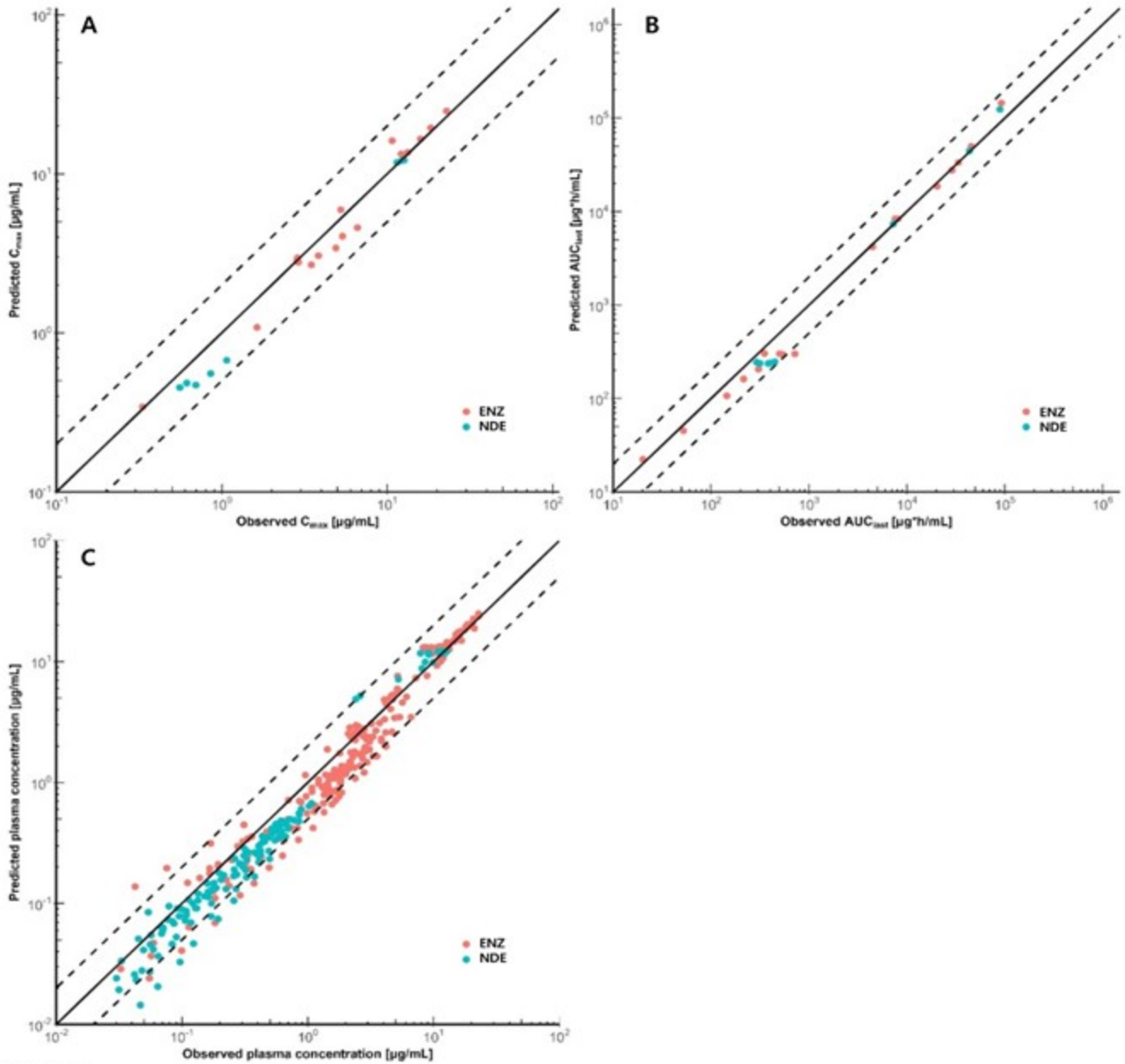


FIGURE 2
Goodness-of-fit plots for the developed PBPK model of enzalutamide and N-desmethyl enzalutamide for the predicted versus observed of (A) C_{max}, (B) AUC_{last}, and (C) plasma concentration. solid line, identification line; dashedline, 2-fold deviation; ENZ, enzalutamide ; NDE, N-desmethyl enzalutamide; ; C_{max}, maximum plasma concentration; AUC_{last}, area under the concentration-time curve from zero to last.

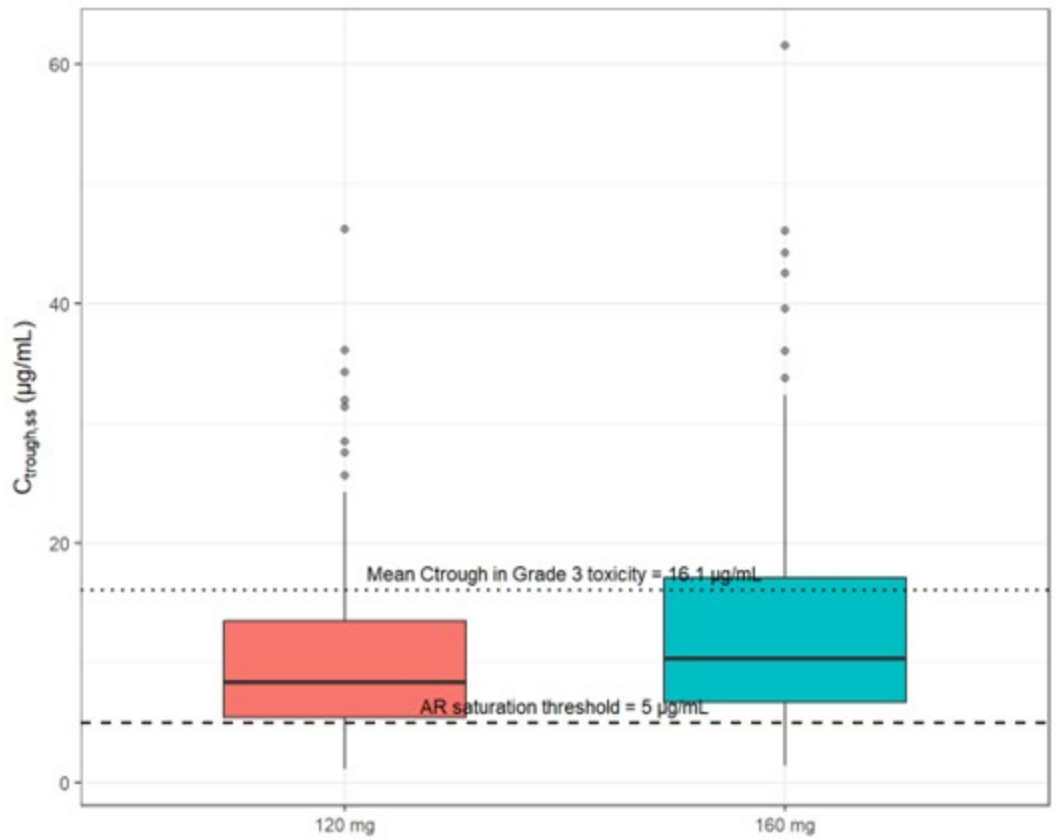


FIGURE 3
PBPK-predicted steady-state trough concentrations ($C_{trough,ss}$) of enzalutamide following once-daily administration of 120 and 160 mg. Dashed and dotted lines indicate the AR occupancy benchmark (5 µg/mL) and exploratory toxicity-associated reference concentration (16.1 µg/mL), respectively.

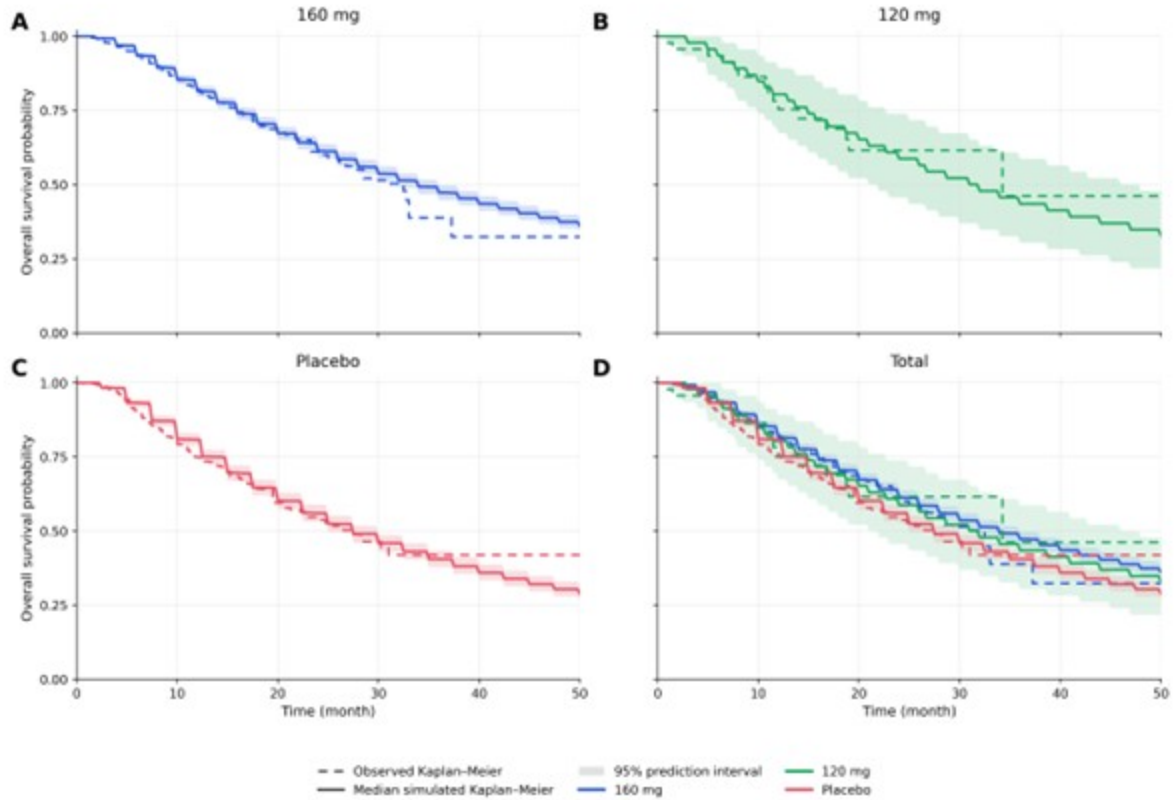


FIGURE 4
Visual predictive check (VPC) for the Overall survival E-R model of (A) 160mg group, (B) 120mg group, (C) Placebo group, (D) combined 160mg, 120mg and placebo group. step line, observed data; linear line, mean of predicted data; ribbon, 95% CI of predicted data.

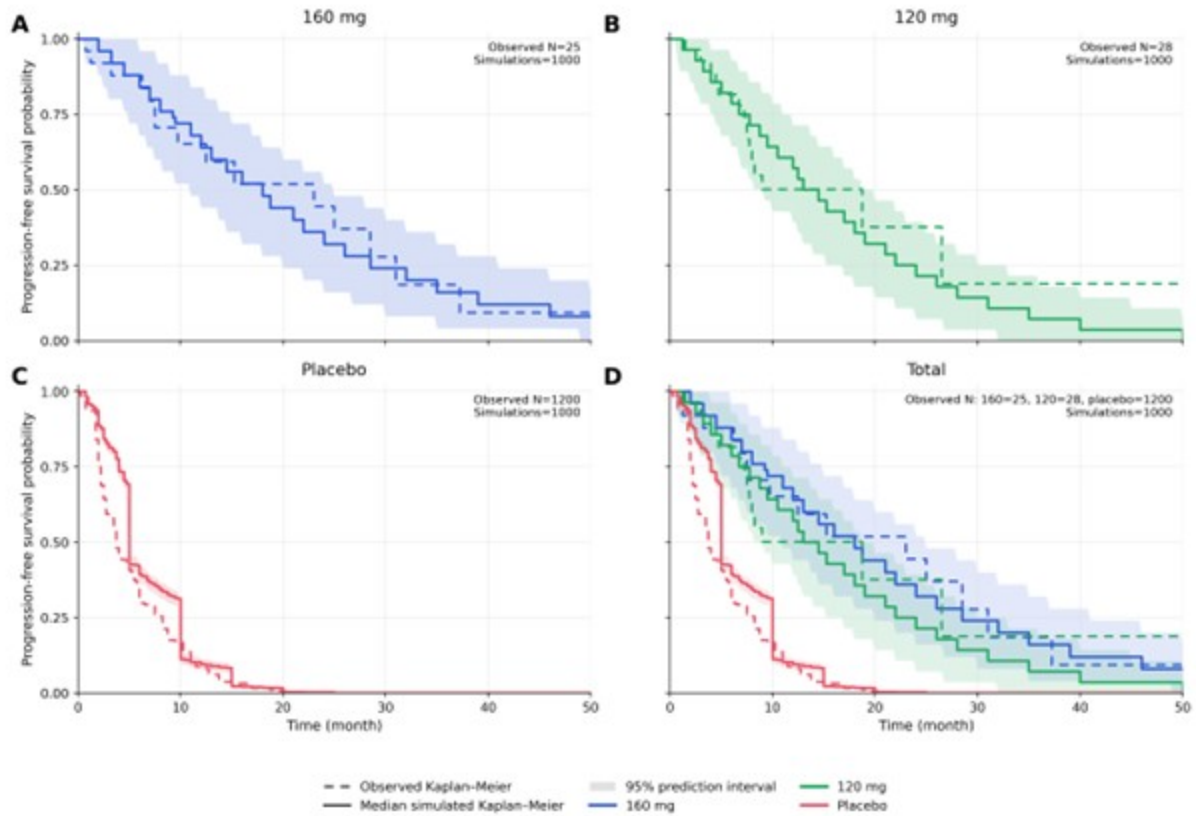


FIGURE 5
Visual predictive check (VPC) for the Progression-free survival E-R model of (A) 160mg group, (B) 120mg group, (C) Placebo group, (D) comb ined 160mg, 120mg and placebo group. step line, observed data; linear line, mean of predicted data; ribbon, 95% CI of predicted data.

Supplementary Files

This is a list of supplementary files associated with this preprint. Click to download.

- Table1.docx
- Table2.docx
- Table3.docx
- SupplementaryMaterialS1.docx